Anion Interactions

DOI: 10.1002/anie.201001755

The π-Accepting Arene $HAT(CN)_6$ as a Halide Receptor through Charge Transfer: Multisite Anion Interactions and Self-Assembly in Solution and the Solid State**

Helen T. Chifotides, Brandi L. Schottel, and Kim R. Dunbar**

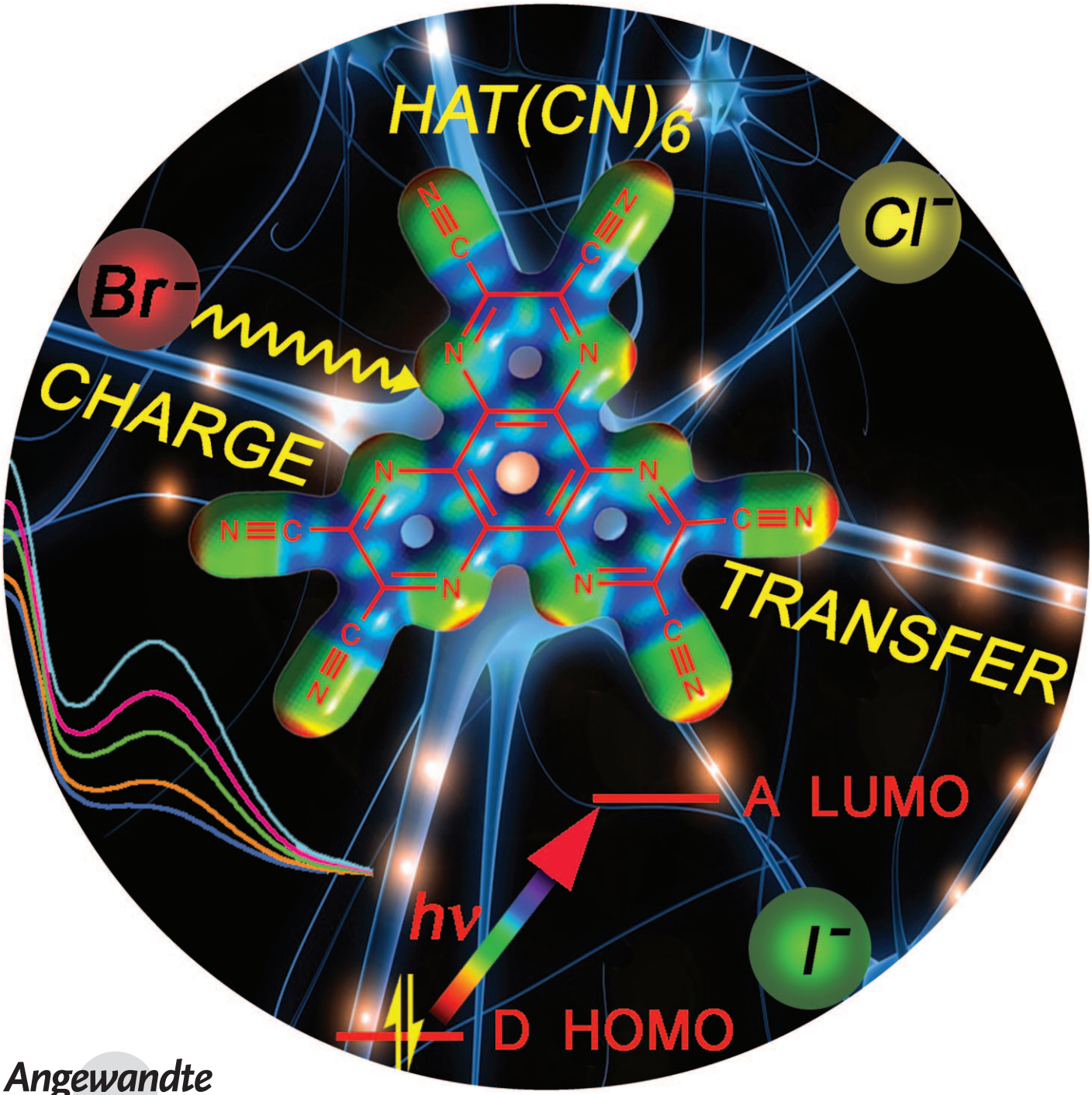

Noncovalent interactions of anions have garnered much interest with the goal to design anion-specific molecular sensors and receptors[1–4] for applications in biological and medicinal chemistry, e.g., transmembrane "anion–π slides".[5] Three independent theoretical studies,[6–8] confirming that the recently recognized noncovalent contacts between anions and charge-neutral electron-deficient aromatic rings, namely, anion–π interactions,[9–11] are attractive, have been complemented by mounting experimental evidence for their existence in the solid state[9,10,12] and in solution.[13–17] For π-acidic arenes such as hexafluorobenzene, the anion typically resides directly over the electron-deficient aromatic ring centroid.[7,8,10,12] In highly electron-deficient arenes, however, e.g., tetracyanopyrazine,[13,18,19] tetracyanobenzene,[20a] and others,[17,20b] X-ray crystal structure determinations and theoretical studies[11,20a,21] reveal that the anion is preferentially located over the periphery of the ring. In the aforementioned systems, the π-acceptor/anion interaction involves charge-transfer (CT),[11,20a] which in several cases is accompanied by the appearance of highly colored solutions or crystals,[13,18,19] rendering them promising candidates for designing selective anion-sensing receptors.[1]

Herein, our studies target an extended π electron-deficient molecular unit with multiple sites available for interactions with anions, namely $HAT(CN)_6$ (**1**) (1,4,5,8,9,12-hexaazatriphenylene-hexacarbonitrile, Scheme 1). The high π-acidity of **1**, due to the conjugated cyano groups, its high molecular polarizability, and positive quadrupole moment, render **1** a particularly attractive heterocyclic system to establish anion- or lone pair–π contacts.[22] Our previous attempts to reduce **1** with $[n\mathrm{Bu_4N}][\mathrm{I}]$ unexpectedly resulted in the isolation of $\{([n\mathrm{Bu_4N}][\mathrm{I}])_3[\mathrm{HAT(CN)_6}]_2\}\cdot 3\,\mathrm{C_6H_6}$ (**2**).[23] The intensely colored crystals of **2** and the low-lying degenerate LUMOs of **1**,[23] which undergoes three reversible redox processes,[22] suggested that indeed **1** has excellent π-accepting capabilities to engage in CT complexes with appropriate electron donors. In light of these observations, we undertook a study of the interactions between **1** and the halide salts $[n\mathrm{Bu_4N}][\mathrm{X}]$ ($\mathrm{X} = \mathrm{Cl^-}$, $\mathrm{Br^-}$, $\mathrm{I^-}$) which were unequivocally confirmed in solution by UV/Vis, ^{13}C, and halogen NMR spectroscopy, in the gas phase by ESI-MS experiments, and in the solid state for the iodide (**2**)[23] and bromide (**3**)[24] isostructural analogues $\{([n\mathrm{Bu_4N}][\mathrm{X}])_3[\mathrm{HAT(CN)_6}]_2\}\cdot 3\,\mathrm{C_6H_6}$,

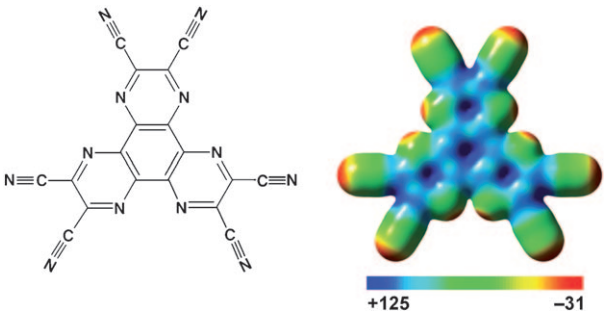

Scheme 1. Structure of **1** and its electron spin polarization (ESP) map [kcal mol^{-1}].

($\mathrm{X^-} = \mathrm{I^-}$, $\mathrm{Br^-}$). The CT complexes of **1** are not only distinctly and intensely colored but also exhibit association constants $K_{CT,X}$ higher by two orders of magnitude as compared to complexes of typical arene acceptors.[13] The features of the halide associates with **1**, stemming from multicentered anion binding in an unprecedented η^2,η^2-fashion, taken together with the exceptional π-acceptor strength of **1** render it a sensitive, selective molecular scaffold for the effective recognition of anions and a promising colorimetric anion sensor. To our knowledge, this is the first study of its type wherein a neutral π electron-deficient aromatic unit is demonstrated to exhibit concomitant multisite anion interactions, namely, both CT and anion–π types, in solution and the solid state; notably, the anions are the driving elements for the self-assembly of the complexes through CT interactions. Additionally, ^{13}C and halogen NMR spectroscopy as well as ES-MS are employed for the first time to detect CT interactions in solution.

The structures of **2**[23] and **3** consist of four layers ABCD that propagate along the *c* axis with units of the π acid alternately interspersed with anions (three or one per layer; Figure 1 a–c). The linear growth of the chains $\{[\mathbf{1}]_2[\mathrm{X}]_3\}^{3-}\cdots[\mathrm{X}]^-\cdots\{[\mathbf{1}]_2[\mathrm{X}]_3\}^{3-}\cdots[\mathrm{X}]^-$ is dictated by contacts between the anions and entities of **1**. The prominent influence of the anions in the packing of **2** and **3** can be appreciated by comparison to the X-ray structure of **1** which does not stack; instead, units of **1** are considerably off-set from one another and form staircase-like or interpenetrating chains.[23] In **2**[23] and **3**, each face of **1** is closely associated with a single anion on one side and three anions on the opposite face with three partially occupied halide ions at the four sites; thus the ratio of **1** to $\mathrm{Br^-}$ or $\mathrm{I^-}$ ions in **2** or **3** is 2:3. The single anion in layer D resides along the axis perpendicular to the benzene centroids and establishes two anion–π contacts with **1** in layers A and C; the distances $d_{X\text{–centr}}$ of each single anion to the centroids of **1** are not equal, nonetheless they are both shorter than the sum of the van der Waals (vdW) R_{vdW} C···X or vdW/ionic R_{ionic} C···X$^-$ radii (Table 1). The vdW contraction for the central ring centroid, $C_{centr} = R_{vdW} - R_{X\text{–centr}}$,[19] for both halides (layer D), is 0.26–0.35 Å (Table 1), which is diagnostic of anion–π interactions in **2** and **3**.[12,18,19] It is notable that $C_{anion\text{–}\pi/I}$ (6%) > $C_{anion\text{–}\pi/Br}$ (3%), an indication of stronger anion–π interactions in **2** due to the higher polarizability of $\mathrm{I^-}$ as compared to $\mathrm{Br^-}$. Furthermore, in **2**[23] and **3**, each of the three equivalent $\mathrm{X^-}$ ions in layer B is located over the periphery of entities of **1** in layers A and C (Figure 1). In

[*] Dr. H. T. Chifotides, B. L. Schottel, Prof. K. R. Dunbar
Department of Chemistry, Texas A&M University
P. O. Box 30012, College Station, TX 77842-3012 (USA)
Fax: (+1) 979-845-7177
E-mail: chifotides@mail.chem.tamu.edu
dunbar@mail.chem.tamu.edu
Homepage: http://www.chem.tamu.edu/rgroup/dunbar/dunbar.htm

[**] We gratefully acknowledge the Welch Foundation (A-1449) and the American Chemical Society Petroleum Research Fund for support of this research (PRF46121-AC3). We also acknowledge Dr. J. Bacsa and Dr. J. H. Reibenspies for their assistance with the X-ray structure solution and refinement. $HAT(CN)_6$ = 1,4,5,8,9,12-hexaazatriphenylene-hexacarbonitrile.

Supporting information for this article is available on the WWW under http://dx.doi.org/10.1002/anie.201001755.

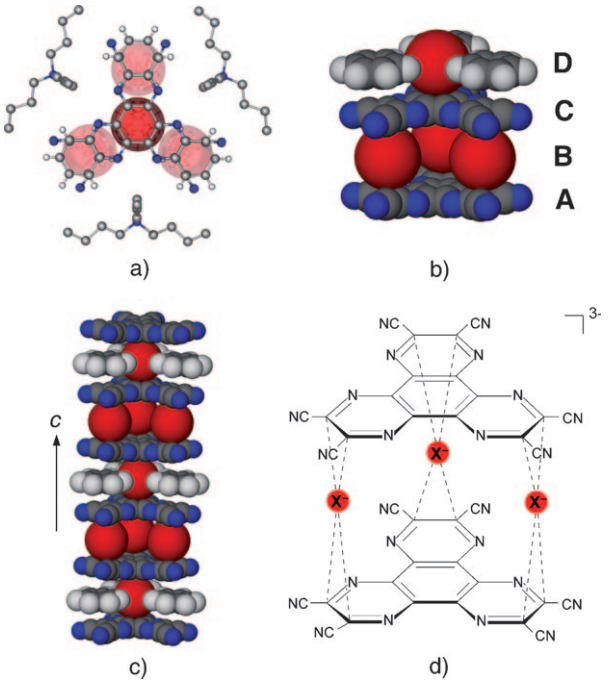

Figure 1. Repeat layers ABCD of **3**: a) down and b) along *c* axis, c) forming 1D vertical stacks (cations omitted for clarity); atom colors: C gray, N dark blue, Br red, H white. d) Multi-site anion contacts with C_{ext} in $\{[\mathbf{1}]_2[X]_3\}^{3-}$.

particular, each anion X^- is equidistant from the pyrazine external carbon atoms C_{ext} of **1**, in an η^2,η^2-fashion (Figure 1d), at distances by up to 0.35 Å shorter than the sum R_{vdW} C···X from layers A and C (Table 1; average contraction factors $C_{R\text{-}CT} \approx 7\%$ point to relatively strong contacts). The observed off-center geometries of the anions, their close contacts to C_{ext}, and the appearance of highly colored solids, all collectively point to dominant CT interactions in **2** and **3**. The shorter distances of the peripheral anions to C_{ext}, as compared to the central anions from C_{int} of the central ring, imply that the anion–π interactions are clearly weaker than the CT contacts in **2** and **3**.[11,20a]

In the UV/Vis solution studies, addition of a colorless solution of $[n\mathrm{Bu_4N}][X]$ ($X^- = I^-$, Br^-, Cl^-) to a yellow solution of **1** in THF induces the spontaneous appearance of new intense absorption bands, that progressively grow with increasing concentration of salt at 630, 419, or 408 nm, respectively (Figure 2a and S4, S5 in the Supporting Information). These bands correspond to the electronic transitions from the HOMO of the electron donors to the low-lying LUMO of acceptor **1**. The transition energies ($h\nu_{CT}$) are directly related to the HOMO→LUMO energy gap of the $[X^-, HAT(CN)_6]$ complexes; for the common acceptor **1**, they increase linearly with the oxidation potential[25] of the donor in the order $Cl^- > Br^- > I^-$ (Figure 3),[13,18,19] which establishes the unequivocal CT nature of the associations. Furthermore, the shift of the λ_{max} for the new absorption band of each halide to a shorter wavelength in CH_3NO_2 (557, 406, and 390 nm for I^-, Br^-, and Cl^-, respectively; Figure 2b, S6, S7) as compared to THF (negative solvatochromism behavior), supports dependence of the transition energies on solvent polarity, which is characteristic of CT bands.

In the Job plots, which are not symmetric, the absorption intensity maxima for the halide complexes with **1**, at ratios $[X^-]/([X^-]+[\mathbf{1}])\times 100 = 60$ (Figure 2, insets), provide evidence of a 2:3 (or 1:1.5) molar stoichiometric ratio of [**1**]:[X^-] in the CT complexes in THF and CH_3NO_2 solutions, which corroborates the solid state ratio for **2** and **3**. Quantitative analyses of the new absorption intensities, as a function of the respective concentration $[X^-]$ were performed to determine the $K_{CT,X}$ and $\varepsilon_{CT,X}$ values of the complexes (Table 2).[26] In both solvents, $K_{CT,Cl} > K_{CT,Br} > K_{CT,I}$, which is in accord with the order of Lewis basicity and thus the electron-donating ability of the donors, $Cl^- > Br^- > I^-$. The $K_{CT,X}$ values for the complexes of **1**, however, are five times higher than those typical of CT complexes ($K_{CT,X} = 1$–$10\,\mathrm{M^{-1}}$)[13] with the same donors in solvents of comparable polarities and, are approximately two orders of magnitude higher in THF ($K_{CT,X} \approx 1\text{–}4\times10^3\,\mathrm{M^{-1}}$). The unusually high $K_{CT,X}$ values, especially in THF, and thus the high stability of the CT complexes of **1** are attributed to its exceptional acceptor strength. Apart from $K_{CT,X}$, the electronic coupling elements H_{CT}[19,27] (Table 2) are directly correlated to the spectral properties and offer a means for evaluating the stabilities of the CT complexes. The H_{CT} values for the complexes indicate considerable orbital interactions in THF which become weaker in CH_3NO_2. In both solvents, however, the H_{CT} values increase in the order $Cl^- > Br^- > I^-$, in accord with the expected increasing orbital overlap with decreasing anion size. In support of the aforementioned contention are the calculated values $K_{CT,X}$ (CH_3NO_2) < $K_{CT,X}$ (THF), which suggest that the position of equilibrium for complex formation is greatly affected by solvent polarity.[28]

The positioning of the halide anions in the associates of **1** was probed in solution by ^{13}C NMR spectroscopy. The aromatic region for each complex in $[D_8]$THF or CD_3NO_2 exhibits three resonances for the peripheral $^{13}C_{ext}$, central $^{13}C_{int}$, and cyano $^{13}C_{CN}$ (Table 3). This indicates that the positions of the halide ions are related by a C_3 rotation axis in the complexes. These findings also suggest that the

Table 1: Intermolecular closest contacts for **2** and **3**.[a]

X^-	$d_{X\text{–}centr}$ [Å]	C_{centr} [Å][b]	X···C_{int} [Å]	$C_{anion\text{–}\pi}$ [%][c]	X···C_{ext} or R_{CT} [Å]	R_{vdW} C···X or R_{ionic} C···X^- [Å]	C_{R-CT} [%][d]
I^-[e]	3.337[f]	0.343	3.635[f]	7	3.334[f]	3.68	9
	3.419[g]	0.261	3.666[g]	6	3.506[g]	3.90	5
	3.378[h]	0.302[h]	3.65[h]	6[h]	3.420[h]		7[h]
Br^-	3.245[f]	0.305	3.543[f]	3	3.239[f]	3.55	9
	3.280[g]	0.270	3.579[g]	2	3.354[g]	3.66	6
	3.262[h]	0.288[h]	3.56[h]	3[h]	3.296[h]		7[h]

[a] Each halide ion in contact with two units of **1**. [b] $C_{centr} = R_{vdW} - d_{X\text{–}centr}$.[19] [c] $C_{anion\text{–}\pi} = (1 - R_{exp}/R_{ionic}) \times 100$; for R_{exp}, the X···C_{int} distance was used; R_{ionic} C···X^- = vdW(C) + ionic radius (X^-).[12,19] [d] $C_{R-CT} = (1 - R_{CT}/R_{vdW}) \times 100$.[19] [e] Ref. [23]. [f] Distance to layer A; η^2-binding to two C atoms (Figure 1d). [g] Distance to layer C; η^2-binding to two C atoms. [h] Average value.

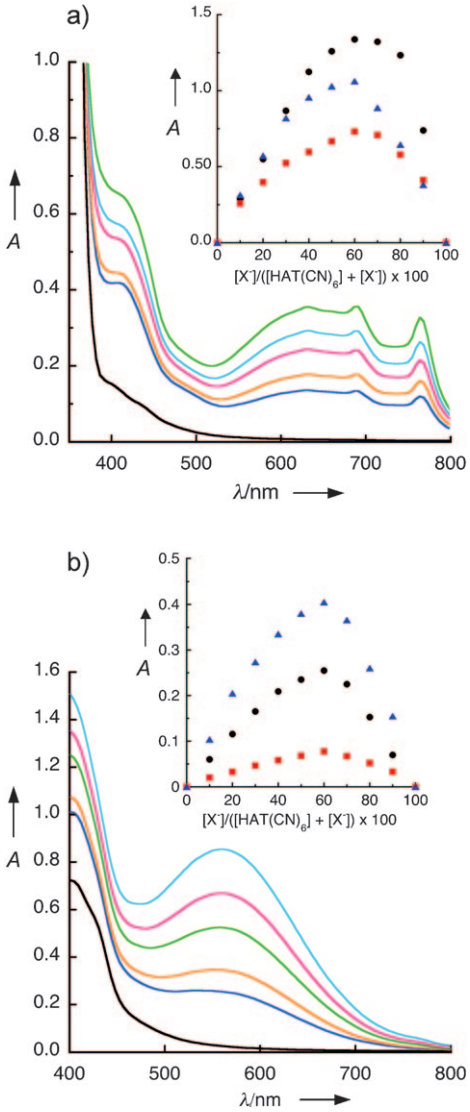

Figure 2. Spectral changes upon addition of [nBu$_4$N][I] solutions to **1** in: a) THF; [nBu$_4$N][I] in mM, line color: 0 (black); 0.311 (blue); 0.463 (orange); 0.776 (red); 1.09 (light blue); 3.55 (green); concentration of **1**: 0.130 mM. b) CH_3NO_2; [nBu$_4$N][I] in mM, line color: 0 (black); 5.54 (blue); 8.27 (orange); 13.8 (green); 19.3 (red); 27.6 (light blue); concentration of **1**: 0.950 mM. Insets: Job plots for **1** with (●) chloride, (■) bromide, and (▲) iodide ions in a) THF; b) CH_3NO_2.

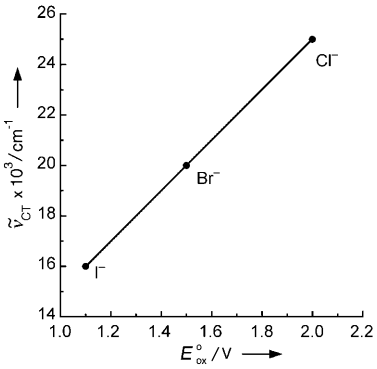

Figure 3. Mulliken dependence of $\tilde{\nu}_{CT}$ for CT complexes of **1** in THF with the oxidation potentials of the halides.

Table 2: Spectroscopic features for halide associates[a] of **1**.

	Cl^-	Br^-	I^-	Solvent
λ_{max} [nm]	408	419	630	[b]
K_{CT} [M^{-1}][c]	3780	2200	940	[b]
ε_{CT} [$M^{-1}cm^{-1}$]	12785	8258	4437	[b]
ΔG_{CT} [kJ mol^{-1}][c]	−20.4	−19.1	−17.0	[b]
R_{CT} [Å][d]	3.14[e]	3.239	3.334[f]	
H_{CT} [10^3 cm^{-1}][g]	5.8	4.5	2.9	[b]
H_{CT} [eV]	0.72[h]	0.55	0.36	[b]
λ_{max} [nm]	390	406	557	[i]
K_{CT} [M^{-1}][c]	71	48	20	[i]
ε_{CT} [$M^{-1}cm^{-1}$]	3513	3354	2481	[i]
ΔG_{CT} [kJ mol^{-1}][c]	−10.6	−9.6	−7.4	[i]
H_{CT} [10^3 cm^{-1}][g]	3.3	2.8	2.2	[i]
H_{CT} [eV]	0.41[h]	0.35	0.27	[i]

[a] As [nBu$_4$N]$^+$ salts. [b] THF. [c] At 25 °C; for K_{CT} estimated relative error ±10%. [d] Shortest distance X···C_{ext} from X-ray data was used (Table 1). [e] Estimated value for Cl^- complex from $C_{R\text{-}CT}$ of **3** (9%) with $C_{R\text{-}CT} = (1-R_{CT}/R_{vdW})\times 100$[19] and vdW radii sum C···Cl = 3.45 Å.[12] [f] Ref. [23]. [g] Refs [19], [27]. [h] Calculated with estimated $R_{CT,Cl}$. [i] CH_3NO_2.

Table 3: ^{13}C NMR resonances [ppm] for **1** and CT associates[a] of **1**.

	$\delta\ ^{13}C_{ext}$	$\Delta\delta_{ext}$[b]	$\delta\ ^{13}C_{int}$	$\Delta\delta_{int}$[b]	$\delta\ ^{13}C_{CN}$	$\Delta\delta_{CN}$[b]	Solvent
1	143.69	–	136.63	–	114.35	–	[c]
Cl^-	144.77	1.08	136.01	−0.62	114.78	0.43	[c]
Br^-	144.52	0.83	136.25	−0.38	114.70	0.35	[c]
I^-	144.4[d]	0.71	136.37[e]	−0.26	114.64	0.29	[c]
1	142.90	–	136.46	–	114.04	–	[f]
Cl^-	145.72	2.82	134.45	−1.95	114.89	0.85	[f]
Br^-	145.47	2.57	134.68	−1.78	114.84	0.80	[f]
I^-	[g]	–	135.61	−0.85	114.81	0.77	[f]

[a] As [nBu$_4$N]$^+$ salts. [b] $\Delta\delta = \delta_{CT\ Complex} - \delta_{HAT(CN)_6}$. [c] CD_3NO_2. [d] Very broad resonance due to proximity of ^{127}I nuclei.[30] [e] Sharp resonance. [f] [D_8]THF. [g] Not observed.[30]

three anions are positioned over the centers of the C_{ext}–C_{ext} bonds of **1** in an η^2 fashion, in agreement with the findings from the solid-state data for **2** and **3** (Figure 1d). Additionally, the same resonances remain in the ^{13}C NMR spectrum of each complex at −60 °C in [D_8]THF which indicates that the ions are not shared among the three C_{ext}–C_{ext} positions at room temperature. The CT interactions of the halides with C_{ext} are also supported by the downfield shifts of the $^{13}C_{ext}$ resonances by $\Delta\delta_{ext} \approx 1$–3 ppm as compared to **1** (Table 3) in both solvents. Despite the expected upfield shift of the $^{13}C_{ext}$ resonances, they move downfield as the C atoms in proximity with the halides become deshielded by their electron-withdrawing effect.[29] Furthermore, the breadth of the $^{13}C_{ext}$ NMR resonance of the iodide complex in CD_3NO_2 and its invisibility (due to severe broadening) in [D_8]THF,[30] indicate proximity of the ^{127}I nuclei to $^{13}C_{ext}$ (Figure 1d). On the contrary, the $^{13}C_{int}$ NMR resonances shift upfield[31] and remain sharp, which precludes halide nuclei above the central ring centroid.

In order to further characterize the CT complexes, halide NMR spectra were collected for [nBu$_4$N][X] ($X^- = Cl^-$, Br^-, I^-) and their complexes with **1** (Table 4). ^{35}Cl, ^{81}Br, and ^{127}I NMR spectroscopy are rarely used and, to our knowledge, have not been previously applied to study CT contacts. The

Table 4: ^{35}Cl, ^{81}Br, and ^{127}I NMR chemical shifts [ppm] of [nBu$_4$N][X] and associates with **1** at 22 °C.

Nucleus	δ for nBu$_4$NX	δ for associates of **1**	Solvent
^{35}Cl	25.8	33.1[a]	[b]
^{81}Br	50.6	63.2	[b]
^{127}I	68.6	84.7[c]	[b]
^{35}Cl	27.3	53.7[c]	[d]
^{81}Br	66.7	117.0[c]	[d]
^{127}I	[e]	[e]	[d]

[a] Single resonance $\delta = 33.4$ ppm remains at −27 °C. [b] CD_3NO_2. [c] Extremely broad. [d] [D$_8$]THF. [e] Data could not be acquired; see Ref. [32].

three halogen nuclei have appreciable nuclear quadrupole moments ($I > 1/2$) rendering NMR data collection particularly challenging, especially in the case of ^{127}I ($I = 5/2$).[30] Despite the issues involved, we were successful in collecting the halogen NMR spectrum of each CT complex,[32] which exhibits a single resonance, shifted considerably downfield with respect to the corresponding free halide ion (Table 4; Figure S9); this is indicative of a single type of halide interaction in each complex and deshielding of the donor nuclei[15] due to CT, thus confirming the structure depicted in Figure 1 d in solution.

The appearance of a single resonance in the ^{35}Cl NMR spectrum, even at −27 °C, further supports CT as the sole interaction between **1** and chloride ions in solution (Figure S10). The downfield shifts of the complex resonances are considerably greater in [D$_8$]THF as compared to CD_3NO_2 (Table 4) due to the lower dielectric constant of THF. In both CD_3NO_2 and [D$_8$]THF, $\Delta\delta(^{35}Cl) > \Delta\delta(^{81}Br) > \Delta\delta$ (^{127}I), which corroborates the strength of the interactions established from $^{13}C_{ext}$ NMR, i.e., $\Delta\delta$ $C_{ext}(Cl) > \Delta\delta$ $C_{ext}(Br) > \Delta\delta$ $C_{ext}(I)$, and the spectroscopic findings (K_{CT}, H_{CT}). The strength of the latter CT interactions is also supported by the unusually high negative values for ΔG_{CT} (Table 2), especially in THF, attributed to the large increase in enthalpy from the multisite CT interactions of each anion (four per anion; Figure 1 d), which compensates for the entropy loss associated with the multi-ion chelate complexation.[28] The negative changes in ΔG_{CT} reflect the spontaneous character of the association which proceeds in solution with formation of $\{[\mathbf{1}]_2[X]_3\}^{3-}$ assemblies. Remarkably, the anions are the directing elements[33] for the self-assembly of the entities, which is unprecedented for CT interactions to our knowledge.

Finally, ES-MS data also provided strong evidence that CT interactions between halide ions and **1** persist in solution and in the gas phase by observation of $\{[\mathbf{1}][X]\}^-$ for ($X^- = Cl^-$, Br^-, I^-) at m/z 419.00, 464.95, and 510.93, respectively (Figures S11–S13). The fact that species such as $\{[\mathbf{1}]_2[X]_3\}^{3-}$ were not detected by ESI-MS is not surprising given the charge repulsion of three negative charges in close proximity in the gas phase. Furthermore, the addition of [nBu$_4$N][X] to any one of the other halide complex solutions in THF resulted in new peaks at m/z 419.00, 464.95 or 510.93, indicating the presence of $\{[\mathbf{1}][X]\}^-$ (Figures S14–S18).

In conclusion, dominant multisite CT interactions, surpassing the typical arene acceptors studied to date, were detected for **1** both in solution and the solid state. In **2** and **3**, the CT interactions in the $\{[\mathbf{1}]_2[X]_3\}^{3-}$ units ($X^- = Br^-$, I^-) are clearly indicated by close η^2,η^2-contacts of the halide ions to the peripheral C_{ext} of **1**. To our knowledge, **1** is a unique case of a π electron-deficient entity that exhibits concomitant CT and anion–π type contacts in the solid state. In solution, the spontaneous formation of $\{[\mathbf{1}]_2[X]_3\}^{3-}$ assemblies, with peripheral η^2,η^2-positioning of the anions and the unambiguous CT nature of the associations with **1** are fully supported by the UV/Vis, ^{13}C, halogen NMR, and ES-MS data. The high stability of the distinctly colored complexes assembled with the anions as directing elements and the simultaneous multisite CT interactions in which **1** engages are unique in the literature of this area and are highly desirable features for the design of anion-sensing receptors. Studies of interactions of **1** with other anions are underway and will be reported in due course.

Received: March 25, 2010
Published online: July 15, 2010

Keywords: anion receptors · anion–π interactions · charge-transfer · donor–acceptor systems · supramolecular chemistry

[1] J. L. Sessler, P. A. Gale, W.-S. Cho, *Anion Receptor Chemistry*, The Royal Society of Chemistry, Cambridge, **2006**.
[2] M. Mascal, I. Yakovlev, E. B. Nikitin, J. C. Fettinger, *Angew. Chem.* **2007**, *119*, 8938; *Angew. Chem. Int. Ed.* **2007**, *46*, 8782, and references therein.
[3] R. Custelcean, J. Bosano, P. V. Bonnesen, V. Kertesz, B. P. Hay, *Angew. Chem.* **2009**, *121*, 4085; *Angew. Chem. Int. Ed.* **2009**, *48*, 4025.
[4] C. Caltagirone, P. A. Gale, *Chem. Soc. Rev.* **2009**, *38*, 520.
[5] a) S. Matile, *Chem. Eur. J.* **2009**, *15*, 28; b) during the galley proof stage of this manuscript, this important reference came to our attention: R. E. Dawson, A. Hennig, D. P. Weimann, D. Emery, V. Ravikumar, J. Montenegro, T. Takeuchi, S. Gabutti, M. Mayor, J. Mareda, C. A. Schalley, S. Matile, *Nat. Chem.* **2010**, *2*, 533.
[6] I. Alkorta, I. Rozas, J. Elguero, *J. Am. Chem. Soc.* **2002**, *124*, 8593.
[7] D. Quiñonero, C. Garau, C. Rotger, A. Frontera, P. Ballester, A. Costa, P. M. Deyà, *Angew. Chem.* **2002**, *114*, 3539; *Angew. Chem. Int. Ed.* **2002**, *41*, 3389.
[8] M. Mascal, A. Armstrong, M. D. Bartberger, *J. Am. Chem. Soc.* **2002**, *124*, 6274.
[9] P. Gamez, T. J. Mooibroek, S. J. Teat, J. Reedijk, *Acc. Chem. Res.* **2007**, *40*, 435.
[10] B. L. Schottel, H. T. Chifotides, K. R. Dunbar, *Chem. Soc. Rev.* **2008**, *37*, 68.
[11] B. P. Hay, V. S. Bryantsev, *Chem. Commun.* **2008**, 2417.
[12] T. J. Mooibroek, C. A. Black, P. Gamez, J. Reedijk, *Cryst. Growth Des.* **2008**, *8*, 1082.
[13] Y. S. Rosokha, S. V. Lindeman, S. V. Rosokha, J. K. Kochi, *Angew. Chem.* **2004**, *116*, 4750; *Angew. Chem. Int. Ed.* **2004**, *43*, 4650.
[14] O. B. Berryman, F. Hof, M. J. Hynes, D. W. Johnson, *Chem. Commun.* **2006**, 506.
[15] D.-X. Wang, Q.-Y. Zheng, Q.-Q. Wang, M.-X. Wang, *Angew. Chem.* **2008**, *120*, 7595; *Angew. Chem. Int. Ed.* **2008**, *47*, 7485.

[16] G. Gil-Ramírez, E. C. Escudero-Adán, J. Benet-Buchholtz, P. Ballester, *Angew. Chem.* **2008**, *120*, 4182; *Angew. Chem. Int. Ed.* **2008**, *47*, 4114.
[17] O. B. Berryman, D. W. Johnson, *Chem. Commun.* **2009**, 3143.
[18] S. V. Rosokha, J. K. Kochi, *Struct. Bonding (Berlin)* **2008**, *126*, 137.
[19] B. Han, J. Lu, J. K. Kochi, *Cryst. Growth Des.* **2008**, *8*, 1327.
[20] a) O. B. Berryman, V. S. Bryantsev, D. P. Stay, D. W. Johnson, B. P. Hay, *J. Am. Chem. Soc.* **2007**, *129*, 48; b) O. B. Berryman, A. C. Sather, B. P. Hay, J. S. Meisner, D. W. Johnson, *J. Am. Chem. Soc.* **2008**, *130*, 10895.
[21] P. Ballester, *Struct. Bonding (Berlin)* **2008**, *129*, 127.
[22] D. Tanaka, S. Masaoka, S. Horike, S. Furukawa, M. Mizuno, K. Endo, S. Kitagawa, *Angew. Chem.* **2006**, *118*, 4744; *Angew. Chem. Int. Ed.* **2006**, *45*, 4628, and references therein.
[23] P. S. Szalay, J. R. Galán-Mascarós, B. L. Schottel, J. Bacsa, L. M. Pérez, A. S. Ichimura, A. Chouai, K. R. Dunbar, *J. Cluster Sci.* **2004**, *15*, 503, and references therein.
[24] Synthesis and detailed X-ray data are available in the Supporting Information. Data for **3**: $C_{102}H_{126}N_{27}Br_3$, space group $R3m$, $a = 27.009(2)$, $b = 27.009(2)$, $c = 13.217(1)$ Å, $\alpha = 90.00$, $\beta = 90.00$, $\gamma = 120.00°$, $V = 8350(1)$ Å^3, $Z = 3$, $R = 0.0724$, $wR(F^2) = 0.1347$ [$I > 2\sigma(I)$], GoF = 1.003; CCDC 741080 contains the supplementary crystallographic data for this paper. These data can be obtained free of charge from The Cambridge Crystallographic Data Centre via www.ccdc.cam.ac.uk/data_request/cif.
[25] L. Eberson, *Acta Chem. Scand. Ser. B* **1984**, *38*, 439.
[26] Each data set was fitted to a 1:1 (ca. 1:1.5 from Job plots) molar stoichiometric ratio of [**1**]:[X^-] by plotting [**1**]/Abs_{CT} vs. 1/[X^-].[27]
[27] See Supporting Information.
[28] H.-J. Schneider, *Angew. Chem.* **2009**, *121*, 3982; *Angew. Chem. Int. Ed.* **2009**, *48*, 3924.
[29] L. M. Hancock, P. D. Beer, *Chem. Eur. J.* **2009**, *15*, 42.
[30] The large nuclear quadrupole moment of halides, especially for ^{127}I ($I = 5/2$) results in enhanced quadrupole relaxation effects and large NMR linewidths; "The Quadrupolar Halides Chlorine, Bromine and Iodine": J. W. Akitt in *Multinuclear NMR* (Ed.: J. Mason), Plenum, New York, **1987**.
[31] Secondary electron density from $^{13}C_{ext}$ interacting with halides induces upfield shifts, e.g., ^{13}C (*p*-C) for C_6H_5Cl at 126 from 128 ppm for C_6H_6. *Structure Determination of Organic Compounds* (Eds.: E. Prestsch, P. Bühlmann, C. Affolter), Springer, Berlin, Heidelberg, **2009**, p. 69.
[32] It was not possible to collect reliable ^{127}I NMR spectra for [nBu$_4$N][I] and its complex with **1** in [D_8]THF, due to solvation shell and polarity effects on the quadrupolar relaxation of ^{127}I,[30] resulting in extremely large NMR line widths, e.g., V. I. Chizhik, I. S. Podkorytov, A. P. Kaikkonen, V. I. Mikhailov, *J. Magn. Reson. Ser. A* **1996**, *123*, 1.
[33] O. B. Berryman, C. A. Johnson II, L. N. Zakharov, M. M. Haley, D. W. Johnson, *Angew. Chem.* **2008**, *120*, 123; *Angew. Chem. Int. Ed.* **2008**, *47*, 117.

